Agricultural Water Management 176 (2016) 191–202

Contents lists available at ScienceDirect

Agricultural Water Management

journal homepage: www.elsevier.com/locate/agwat

A water harvesting model for optimizing rainwater harvesting in the wadi Oum Zessar watershed, Tunisia

Ammar Adham[a,d,*], Jan G. Wesseling[a,b], Michel Riksen[a], Mohamed Ouessar[c], Coen J. Ritsema[a]

[a] Wageningen University, Soil Physics and Land Management Group, P.O. Box 47, 6700 AA Wageningen, The Netherlands
[b] Wageningen University and Research Center, Alterra, Soil, Water and Land Use Team, P.O. Box 47, 6700 AA Wageningen, The Netherlands
[c] Institut des Régions Arides, Route de Djorf km 22.5, 4119 Medenine, Tunisia
[d] University of Anbar, Ramadi, Iraq

ARTICLE INFO

Article history:
Received 21 December 2015
Received in revised form 30 May 2016
Accepted 4 June 2016
Available online 17 June 2016

Keywords:
Arid and semi-arid regions
RWH
Water-balance
Optimizing
Tunisia

ABSTRACT

Rainwater harvesting (RWH) techniques have been adapted in arid and semi-arid regions to minimise the risk from droughts. The demand for water has increased but water resources have become scarcer, so the assessment and modelling of surface water related to RWH in catchments has become a necessity. An understanding of the hydrological processes at the sub-catchment level is generally lacking, and little attention has been given to the assessment of RWH after implementation. The objective of this study was to develop a simple but generally applicable water-harvesting model and test it at sub-catchment level to evaluate and optimize the performance of RWH under different design and management scenarios. The model was applied to rainfall data for 1980–2004 in 25 sub-catchments of the watershed of Wadi Oum Zessar (south-eastern Tunisia). The performance and analysis of RWH in three types of years (dry, normal, and wet) are presented and discussed. This study emphasises the advantages of simulating long-term water balances at the sub-catchment level for improving our understanding of hydrological processes in the RWH system and provides several solutions for optimizing RWH performance in various scenarios. Changing the spillway heights together with the flow directions had a significant impact on the performance of RWH by making 92% of all sub-catchments supply sufficient water for crop requirements, compared to 44% of the sub-catchments in case of no changes.

1. Introduction

The pressure on water resources is increasing due to climate change and growing demands for water for agricultural and urban development. Aridity and climatic uncertainty are the major challenges faced by farmers in arid and semi-arid regions. These regions have low average annual rainfalls and a highly variable temporal and spatial rainfall distribution. Inhabitants of dry areas have constructed and developed several techniques of rainwater harvesting (RWH) for increasing the availability of water for crop and cattle production.

RWH is a method for inducing, collecting, storing, and conserving local surface runoff for agriculture in arid and semi-arid regions (Gupta et al., 1997). Understanding the performance of RWH, the water yield of a catchment, and the flood flows for planning the structures for harvesting rainwater are amongst the most important objectives of hydrological engineers. RWH structures are designed to catch as much of the expected runoff as possible in a specific recurrence interval while satisfying the water requirements of crops/trees (Adham et al., 2016). RWH must balance water requirements and storage capacity (structure design). Understanding the relationship between rainfall and runoff in catchments is thus necessary. Studying the water balance can provide insights into the hydrological behaviour of catchments and RWH structures and can help to identify the dominant hydrological processes (Uhlenbrook et al., 2008). The water-balance equation presents the values of inflow, outflow, and the change in water storage for an area or water body (Tadesse et al., 2010). Thornthwaite (1948) published the first monthly water balance, and the method has since been adapted, modified, and used in numerous studies (e.g. Gabos and Gasparri 1983; Xu and Vandewiele 1992; Arnell, 1992). Durbude and Venkatesh (2004) applied the Thornthwaite and Mather (TM) models with remote sensing and a Geographic

* Corresponding author at: Wageningen University, Soil Physics and Land Management Group, P.O. Box 47, 6700 AA Wageningen, The Netherlands.
E-mail addresses: ammar.ali@wur.nl, engammar2000@yahoo.com (A. Adham).

http://dx.doi.org/10.1016/j.agwat.2016.06.003
0378-3774/

Information System (GIS) to identify potential zones of runoff and suitable sites for RWH in Africa, such as contours, farm ponds, gully plugs, and percolation tanks. Jasrotia et al. (2009) applied the TM models with remote sensing and a GIS to understand the water balance of RWH structures in the Devak-Rui watershed in India.

Budyko (1974) developed an empirical relationship between the ratio of mean annual evaporation, rainfall and dryness index of the catchment to analyse the catchment water balance (Gebrekristos, 2015). Budyko's framework has been widely applied in the catchments around the world (Donohue et al., 2006; Gebrekristos, 2015; Potter and Zhang, 2009; Yang et al., 2009). Yang et al. (2007) analysed the spatiotemporal variability of annual evaporation and runoff for 108 catchments in China and explored both regional and inter-annual variability in annual water balance. Tekleab et al. (2011) applied water balance to analyse twenty catchments in the Upper Blue Nile using top-down modelling based on Budyko's hypotheses for temporal and spatial scales.

Rainfall is the most important term in the water balance equation, so the interpretation of past records of rainfall and hydrological events in terms of future probabilities of occurrence is one of the challenges for engineers designers and hydrologists. Analysis of maximum rainfall over a catchment area at different frequencies or return periods is a basic tool for safe and economic planning, management of water resources applications and designing of hydraulic structures (Bhakar et al., 2008; Chow et al., 1988; Durbude, 2008). Probability and frequency analysis of rainfall data can be applied to obtain predicted amounts of precipitation for various probabilities (Bhakar et al., 2008). Similar analysis techniques can be applied to predict maximum daily rainfall of future events from the available data (Kumar and Kumar, 1989). Frequency analysis of rainfall is a tool for solving various water management problems (Kumar et al., 2007). Therefore, the probability and frequency of the occurrence of future events of rainfall can be used to minimise flood risks and periods of drought, and for planning and designing of water resources related to engineering such as small dams, reservoirs, culverts, drainage works, and rainwater harvesting structures (Dabral et al., 2009).

An understanding of the hydrological processes at the sub-catchment level is generally lacking in practice. Relatively, little attention has been paid to the evaluation of RWH systems after implementation. Few studies have investigated the effectiveness of catching and storing water and the utility of RWH within the existing land use and farm management. The objective of the study was to develop a simple but generally applicable water-harvesting model and apply it at sub-catchment level to evaluate and optimize the performance of RWH under different design and management scenarios. The target was to improve water availability for different RWH systems based on crop water requirements, the rainfall-runoff relationship, and the design of RWH structures.

2. Materials and method

2.1. Study area

A 50 ha catchment in an upstream area of the Wadi Oum Zessar watershed in south-eastern Tunisia was selected for the case study. The watershed has a surface area of 367 km^2, and the catchment consists of 25 sub-catchments (Fig. 1). The area has an arid Mediterranean climate, with an average annual rainfall of 150–230 mm, an average annual temperature of 19–22 °C, and an average annual potential evapotranspiration of 1450 mm (Adham et al., 2016; Ouessar, 2007).

Farmers in the study area have built two types of RWH structures for satisfying the water requirements for rainfed annual crops (cereals and legumes) and trees (mainly olive): jessour (in medium to high slopes areas) and tabias (in gently-sloping foothill areas). Each jessr (singular of jessour) or tabia consists of three parts: an impluvium or catchment area providing the runoff, a terrace or cultivated area where the runoff is collected and crops or trees are grown, and a dyke to catch the water and sediment. Each dyke has a spillway (*menfes* if the spillway is on one or both sides, and *masref* if the spillway is in the middle of the dyke) to regulate water flow between dykes (Fig. 2).

2.2. Data collection

Time-series of daily rainfall records for a period of 25 years (1980–2004) were collected from the Institute des Régions Arides (*IRA*) in Tunisia. They concern seven rain gauge stations:Ben Khedache, Toujan Edkhila, Allamat, Koutine, Sidi Makhlouf, Ksar Hallouf, and Ksar Jedid. Annual maximum daily rainfall was extracted from these data and using statistical techniques for data analysis. Other data were collected from field measurements in the watershed as explained in the next sections.

2.2.1. Catchment characteristics

Physical characteristics (e.g. catchment area, retention area, cropping area, and RWH structural dimensions) were measured for each sub-catchment. All areas, dimensions of the RWH structures, and heights of the existing dykes and spillways for each site were measured by measuring tape and the Global Positioning System (GPS). The total volume of water that could potentially be collected behind each dyke was calculated from these measurements.

To obtain soil textural data from the catchment, each sub-catchment was sampled in different sites (1–3 samples for each site, based on the size of sub-catchment) and depths up to 1.3 m. The samples were taken to the IRA laboratory and analysed. The slope of each sub-catchment was obtained from the DEM (30 m resolution) using ArcGIS 10.0.

A limitation of this study is that, just like in most arid and semi-arid regions, there are no measured runoff data available. Therefore we drew our conclusions about the model performance from field observations and interviews with farmers. Based on these sources, we noticed that some sub-catchments (e.g. 10 and 15) were abandoned and some trees were dead, while other sub-catchment's trees are growing well (e.g. 20 and 22). The main reasons for that are lack of water and unequal distribution of rainwater between these sites.

Field measurements and observation status of 25 sub-catchments are presented in Table 1. In this table a value of one (poor), two (medium) or three (well), was assigned to each sub-catchment, based upon field observations and farmers interviews. The function status represents the efficient work of each structure (collected and storage rainwater), production yield, trees growing and the relation between up and downstream. Whereas, maintenance is related to the structure such as restoring the spillway height after each storm, keeping the dam in shape and removing the obstacles that block the main waterway.

2.2.2. Measurements of infiltration rate

The infiltration rate was determined using a double-ring infiltrometer (Al-Qinna and Abu-Awwad, 1998). Based on previous field measurements conducted by Bosch et al. (2014) in the same region, we used infiltrometers of two sizes: small (18/30 cm inner-/outer-ring diameter) and large (32/51 cm). Generally, two measurements took place for each site to ensure reliable results. The small infiltrometers were used at least once in each sub-catchment, but the large infiltrometers were used in only 11 sub-catchments because the measurements required much more water. The infiltration rates were measured on the retention (terrace) basin in each sub-catchment. The rings were driven 5–10 cm into the ground carefully

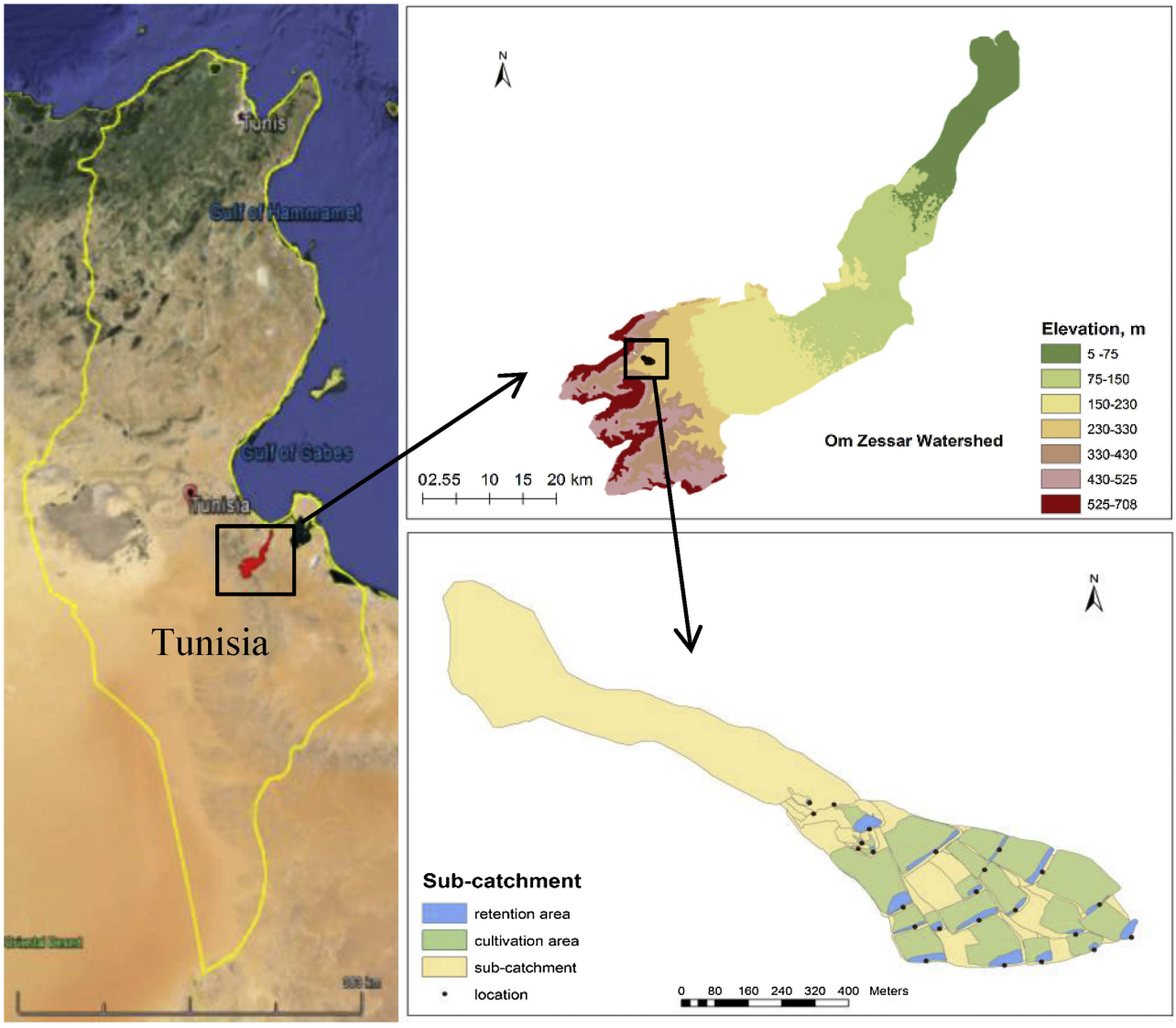

Fig. 1. Location of Wadi Oum Zessar and the test sub-catchment.

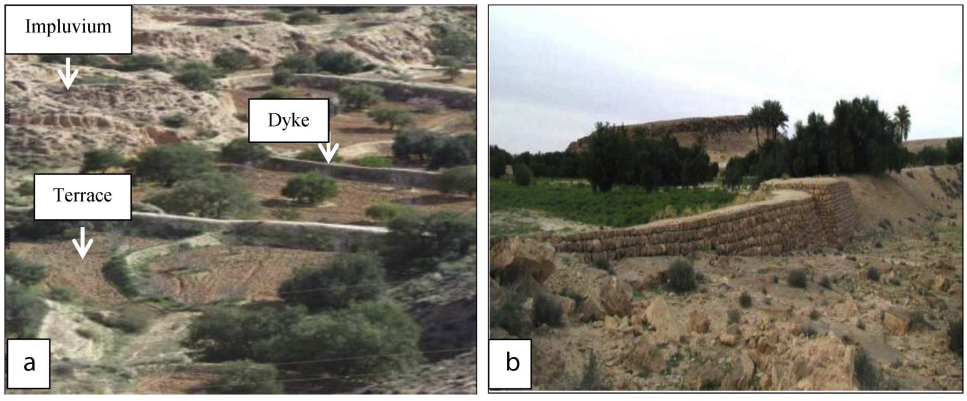

Fig. 2. (a) An example of the jessour (Ouessar, 2007); (b) an example of a spillway.

because the soil contained rocks that might damage the rings or disturb the soil profile. Tap water was used during measurements. The temperature was estimated to vary between 25 and 37 °C. The inner and outer rings were initially filled to a depth of 15 cm. The water level during the test was recorded as a function of time from a scale fixed to the inner ring, and when the level of water in the outer ring dropped below the level in the inner ring, more water was added to maintain equal levels. We continued this procedure until the water level dropped below 5 cm, then the water was replenished for the next repetition. Generally, 1–4 repetitions were done to be

sure that a constant infiltration rate was reached. A plastic bottle or bag was placed inside the rings to prevent disturbing the soil when pouring the water into the rings. From these measurements, the average infiltration rate for a given time period was estimated for each sub-catchment.

2.2.3. Rainfall simulation and the runoff coefficient (C)

A total of 38 rainfall simulations were performed on the impluvium (runoff) areas of the sub-catchments using a Kamphorst's rainfall simulator. Rainfall simulators are devices that imitate the physical characteristics of natural rainfall as close as possible (Aksoy et al., 2012). Kamphorst simulator is small, easy to transport, economic, and has a low water consumption. The device was calibrated as described by Kamphorst (1987). Each test measured water level for three minutes, reading the water level every 30 s. Any runoff was collected in a tube, and the volume was recorded. The value of C (according to the definition of the Food and Agriculture Organization of the United Nations, C is defined as "*runoff divided by the corresponding rainfall both expressed as depth over catchment area (mm)*" (http://www.fao.org/docrep/u3160e/u3160e05.htm) for an individual rainstorm) was calculated for each sub-catchment at the end of each simulation.

2.3. Rainfall probability

Probability analysis can predict maximum daily rainfall of future rain events from the available data with the help of statistical methods (Bhakar et al., 2008; Kumar and Kumar, 1989). The probability distributions most commonly used are the log-Pearson Type-III, log-normal, gamma, and Normal distribution (Kumar et al., 2007; Lee, 2005; Sharma and Singh, 2010). None of the procedures for predicting daily maximum rainfall has been widely accepted (Barkotulla et al., 2009). We analysed the annual maximum daily rainfall data for 1980–2004 to determine the probable maximum daily rainfall for various return periods (T) by a normal distribution function. The RAINBOW program (Raes et al., 1996) was used for frequency analysis, determining the expected rainfall for various probabilities or T values, evaluating the goodness of fit, and testing the homogeneity of the data sets. When dealing with a normal distribution, it is common practice to transform data that are not normally distributed (as in our case) so that the resulting normalized data can be presented by the normal curve. The transformation of the data will change the scale of the records. For positively skewed data a transformation was used to reduce higher values by proportionally greater amounts than smaller values. This transformation rescaled the magnitude of the records and the transformed data became closer to the normal distribution than the original data. Operators available in RAINBOW to rescale the data are the square root, the cubical root and the logarithm. RAINBOW is freely available, and an installation file and reference manual can be downloaded from http://www.biw.kuleuven.be/lbh/lsw/iupware/index.htm. The user can select a distribution type (e.g. normal, log-normal or Weibull) and use graphical methods to obtain a probability plot and histogram of the data.

2.3.1. Probability of exceedance (P_e) and return period T

Let P_e represent the probability of a rainfall greater than a given value. It can be expressed as a percentage. In our study, P_e was estimated using the Weibull method (Weibull, 1939):

$$P_e = \left(\frac{r}{n+1}\right) \times 100 \quad (1)$$

where r is a rank number and n is the number of observations.

Assuming T represents the number of years in which the annual observation is expected to return, then

$$T = {}^{1}\!/\!_{P_e} \quad (2)$$

Rainfall values for selected values of P_e and T were estimated by a frequency analysis using RAINBOW. The probability of future rains can be used to minimise the risks of floods and droughts and for planning and designing structures to optimize the water resources, such as small dams, reservoirs, culverts, drainage channels, and RWH structures (Chow et al., 1988; Dabral et al., 2009).

2.4. Water-harvesting model

The water balance of the 25 water harvesting reservoirs (sub-catchments) was analysed based on the crop water requirements (demand), the rainfall-runoff relationship (supply), and the design of the RWH structures (storage). The change of water storage within the volume was calculated as the difference between total input and output. A catchment generally consists of two main elements: a runoff area and a retention area (reservoir). We analysed the water balance of these two elements and amongst other sub-catchments and assessed the performance of RWH in the entire system to improve the yield of the RWH system. We considered two cases. The first case (Case 1) assumed no relationship between the water flow of the sub-catchments, which are stand-alone units, for two main reasons. Firstly, some sub-catchments receive no upstream water. Secondly, assessing each sub-catchment separately will show the farmers how RWH works. For example, if the amount of water exceeds the storage capacity, the farmer can improve the storage area or increase the cropping area. The second case (Case 2) considered the interaction between the sub-catchments for analysing the relationship between up- and downstream sub-catchments.

The water-balance equation of an area can be written in units of volume (m^3) as:

$$\Delta S = I - Q \quad (3)$$

(Boers et al., 1986) where ΔS is the change in storage during a defined period of time, I is the inflow, and Q is the outflow, all in m^3.

Recognition of the various types of in-and outflow allows a more detailed water-balance equation:

$$\Delta S = Q_{runoff} + Q_{rain\ fall} + Q_{in} - Q_{out} - Inf - ET_c \quad (4)$$

where Q_{in} is the volume of inflow from upstream catchment(s), Q_{out} is the volume of overflow from the retention basin to the next catchment(s), Inf is the infiltration loss from the retention basin obtained from the measured infiltration rate in each sub-catchment using the double-ring infiltrometer, ET_c is the maximum crop evapotranspiration, Q_{runoff} is the volume of runoff into the retention basin from the impluvium (runoff area) calculated as:

$$Q_{runoff} = 0.001 \times C \times P \times A_r \quad (5)$$

where C is the mean annual runoff coefficient (-) measured in the field with the rain simulator. Due to the limited time of our field work, we could not install a gauge station, so no measured runoff-data is available. Therefore we assumed that C of a rainfall event (average simulated) equals the annual average C.

P is the annual precipitation (mm), and A_r is the impluvium or runoff area (m^2), and where $Q_{rainfall}$ is the rainfall in the retention basin, calculated as:

$$Q_{rain\ fall} = 0.001 \times P \times A_b \quad (6)$$

where A_b is the area of the retention basin (m^2).

ET_c was derived from the study conducted by Schiettecatte et al. (2005) for the same watershed. These authors used data

Table 1
Field measurements and observation status of different catchments.

Catchment No	Catchment area (m^2)	Retention area (m^2)	Cultivated area (m^2)	No. of trees	Spillway height (m)	Infiltration rate (mm/h)	Runoff coefficient (C)	Status	
								Function	Maintenance[a]
1	1240	15	20	1	0.60	96	0.21	2	1
2	1412	17	17	1	0.10	101	0.20	2	2
3	1148	119	119	4	0.50	108	0.18	2	1
4	193,249	0	17	7	0.00	18	0.37	1	1
5	11,288	2136	4111	45	0.55	24	0.30	3	3
6	2447	80	244	4	0.50	112	0.30	1	1
7	390	35	154	2	0.45	84	0.29	1	1
8	2756	120	1002	7	0.35	72	0.26	1	1
9	29,160	2079	19,617	105	0.80	103	0.36	2	2
10	5290	521	4107	14	0.40	103	0.36	1	1
11	10,646	1600	9484	30	0.50	108	0.22	2	2
12	22,906	1324	16,855	13	0.40	111	0.18	3	2
13	5953	562	6647	10	0.20	104	0.12	2	2
14	7389	0	4993	0	0.00	102	0.17	1	1
15	8243	478	2658	8	0.30	106	0.34	1	1
16	21,634	1561	9708	20	0.45	60	0.24	1	1
17	4432	518	1646	8	0.40	48	0.18	1	1
18	23,413	2392	14,812	37	0.70	90	0.12	2	2
19	10,307	0	8553	3	0.00	48	0.30	1	1
20	11,651	1548	12,094	28	0.60	101	0.15	3	3
21	19,392	0	20,815	22	0.00	108	0.10	2	1
22	12,664	415	8060	21	0.20	107	0.28	3	3
23	4842	929	4151	18	0.60	108	0.20	2	2
24	7989	317	4224	10	0.50	100	0.15	3	2
25	13,183	1273	8941	15	0.30	110	0.30	3	3

[a] Function and maintenance have a scale from 1 (poor), 2 (medium) and 3 (well) based on the field observations and interviews with local farmers.

from the meteorological station at Medenine and applied the Penman-Monteith method to calculate the average yearly potential evapotranspiration (PET) for 1985–1995. The maximum crop evapotranspiration (ETc) was calculated based on the PET values and the crop coefficient k_c. In case the soil moisture content is insufficient to reach ETc, the actual evapotranspiration (ETa) will be lower than ETc then ETa was estimated for the dominant soil types and applied through the calculation of water balance. To calculate the ETa, the equation Aboukhaled et al. (1975) was used.

The maximum ET_c was calculated by:

$$ETc = PET \times k_c \quad (7)$$

The values for PET, ET_c, and k_c for olive trees are presented in Table 2.

2.4.1. The water harvesting at catchment level (WHCatch) model

As all input data were already stored and available in Excel, so we developed a simple Visual Basic for Applications (VBA) macro in Excel. This macro performed the calculations described above and stored the resulting values in the corresponding cells. The code consisted of a WHCatch module and a Sub-catchmentClass class module. The latter contained all the properties of a sub-catchment and routines to perform some basic computations. The WHCatch module consisted of some private subroutines and three public subroutines. Common users of the Excel workbook will not see the VBA macro. Entering the coding region will only be necessary when new functionality is required. All output is stored and visualised in the same Excel workbook, and the data obtained with this program can be read into a GIS application. The shape file with the layout of the area and the identification numbers (IDs) of the sub-catchments is available in most cases. The sub-catchment ID in the shape file can thus be coupled with the ID in the Excel workbook.

3. Results and discussion

3.1. Infiltration rate and C

The infiltration rate of each considered sub-catchment is presented in Table 1. It can be seen that sub-catchment 6 had the highest infiltration rate (112 mm/h) and sub-catchment 4 had the lowest (18 mm/h), and the average rate was 89 mm/h (Table 1).

Soil type is an important factor affecting the infiltration rate. Sandy loam soil has the highest infiltration rates due to the fact that it has a coarse texture and large pores which promote fast infiltration, while sandy clay and loamy clay have a medium to fine texture. Gregory et al. (2005) obtained infiltration rates above 100 mm/h and less than 50 mm/hour in coarse texture and medium to fine soils, respectively. These infiltration rates are comparable to the ones obtained in the current study where most of the sub-catchments had a sandy loamy soil (as seen from the soil sampling analysis). Moreover, the infiltration rates from our study agreed well with those reported by Makungo and Odiyo (2011), who determined the rates for various soil types in South Africa. Their infiltration rates for sandy loamy soil ranged between 50 and 110 mm/h. Our results, however, differed slightly from those by Bosch et al. (2014), who used double-ring infiltrometers in southeastern Tunisia throughout a wadi with a rocky bed and obtained an average infiltration rate of 65 mm/h. This difference may have been due to the flatness of the jessour/tabias area, so the soil may have been deeper in our retention areas than in the wadi bed. In addition, sub-catchment 4 with the lowest infiltration rate had a relatively steep slope and so suffered from floods and erosion.

The Kamphorst simulator was used for the simulation of rainfall in each impluvium (runoff area) in each sub-catchment. Only the borders of the delineated experimental area were disturbed during the experimental setup. The results from the Kamphorst simulator would thus correspond well to those obtained under field conditions and so are appropriate for RWH calculations for an impluvium. The runoff coefficient C for each subcatchment is shown in Table 1. The maximum value of C was 0.37, measured in an upstream area of sub-catchment 4 where the slope was relatively steep, and the minimum C of 0.10 was measured in sub-catchment 21. The average C was 0.24. The larger values correspond to higher runoff and lower infiltration rates. Moreover, our analysis indicates that the catchment with a large slope usually has a high value of C. Wainwright, 2002 and Zhang et al., 2014 indicate that C is proportional to the slope because fast flow occurs in the steep hillslope area where less

Table 2
Rainfall, potential evapotranspiration (PET), maximum crop evapotranspiration (ETc), and olive crop coefficient k_c (after) (Schiettecatte et al. 2005).

Month	Rainfall (mm)	PET (mm)	ET_c (mm)	k_c for olive
January	37.5	69.6	27.8	0.40
February	30.6	88.6	35.4	0.40
March	40.0	121.2	66.7	0.55
April	16.3	159.3	79.6	0.50
May	11.2	198.4	89.3	0.45
June	1.00	213.5	85.4	0.40
July	0.00	234.8	82.2	0.35
August	2.00	220.9	77.3	0.35
September	17.1	166.6	75.0	0.45
October	23.0	126.8	63.4	0.50
November	19.9	91.1	41.0	0.45
December	36.7	67.4	26.9	0.40

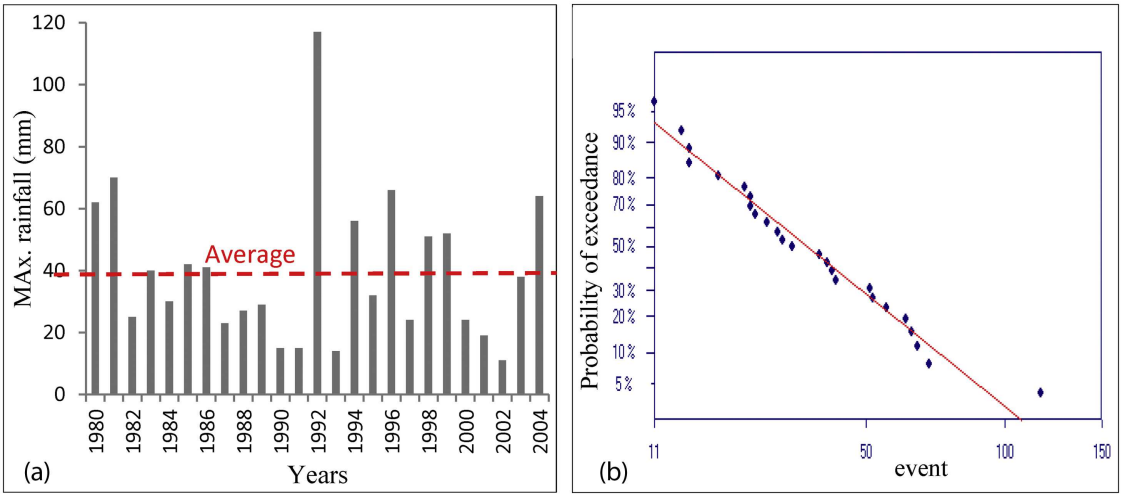

Fig. 3. Annual maximum daily rainfall for 25 years (1980–2004) (a), and the probability analysis of the rainfall data by RAINBOW, showing the rainfalls in mm vs the percentage of probability of exceedance (b).

water remains in the soil or fracture for evapotranspiration. On the other hand, there is a low correlation between C and the size of the catchment area. The runoff measurements agreed well with the above infiltration measurements: sub-catchment 4 had the lowest infiltration rate (18 mm/h) and the highest C (0.37), and sub-catchment 21 had one of the highest infiltration rates (108 mm/h) and the lowest C (0.10) (Table 1). Total rainfall was not significantly correlated with C. These results are in good agreement with those by Schiettecatte et al. (2005) in the Oum-Zessar watershed, where C ranged between 0.002 and 0.841 for initially dry and wet soil conditions.

3.2. Rainfall probability analysis

Daily rainfall data for 1980–2004 were analysed to estimate the design rainfall. Most rains are brief but intense. The minimum daily rainfall was 11 mm in 2002, the maximum was 117 mm in 1992, and the average annual maximum daily rainfall was 39.5 mm (Fig. 3 a,).

The results of the probability analysis using RAINBOW with Weibull's method to calculate the probability is shown in a probability plot (Fig. 3b). The rainfalls corresponding to various P_e's were easily derived from the probability plot by fitting a straight line through the points. A coefficient of determination (R^2) of 0.97 indicated a good fit.

The number of years in which the annual observation is expected to return T (also called the recurrence interval) which is the average time between successive years with the specified rainfall was calculated using RAINBOW too. Various interval probabilities (10, 5, 2, and 1%) can be easily selected in RAINBOW. The estimates of rainfall for the selected probabilities or T's are then obtained from a frequency analysis. The user can also specify a specific rainfall or T and obtain the corresponding T or specific value. For example, if the threshold rainfall is 28.7 mm, then the estimated T will be 1.63 years. The design rainfall will decrease as the probability level increases, and vice versa. For instance, there was 90% chance of receiving 13 mm of rainfall (once every year), whilst the chance of receiving 75 mm was only 10% (once every 10 years).

3.3. The water-harvesting model (WHCatch)

The WHCatch model was applied for several rainfall events over 25 years in the 25 sub-catchments, then the threshold rainfall was determined which represents which events must be reached to generate stream flow (over flow between sub-catchments). The maximum daily rainfall was 117 mm in 1992, and the threshold rainfall was 28.7 mm. The T's for the maximum and threshold rainfalls were about 90 and 1.63 years, respectively. Runoff differed greatly amongst the sub-catchments between two rains (Fig. 4).

The highest rainfall (117 mm) produced a large amount of runoff (Fig. 4a), but the amount was not considered consequential because this amount of rain may fall only once every 90 years. The threshold rainfall produced no runoff between sub-catchments (Fig. 4b), except for the broken sub-catchments (4, 14, 19, and 21) and for sub-catchment 5, which was affected by sub-catchment 4. Moreover, the water requirement for crops had a large deficit. The model was thus applied annually for a long term (25 years), and the results for a dry, normal, and wet year (minimum, average, and maxi-

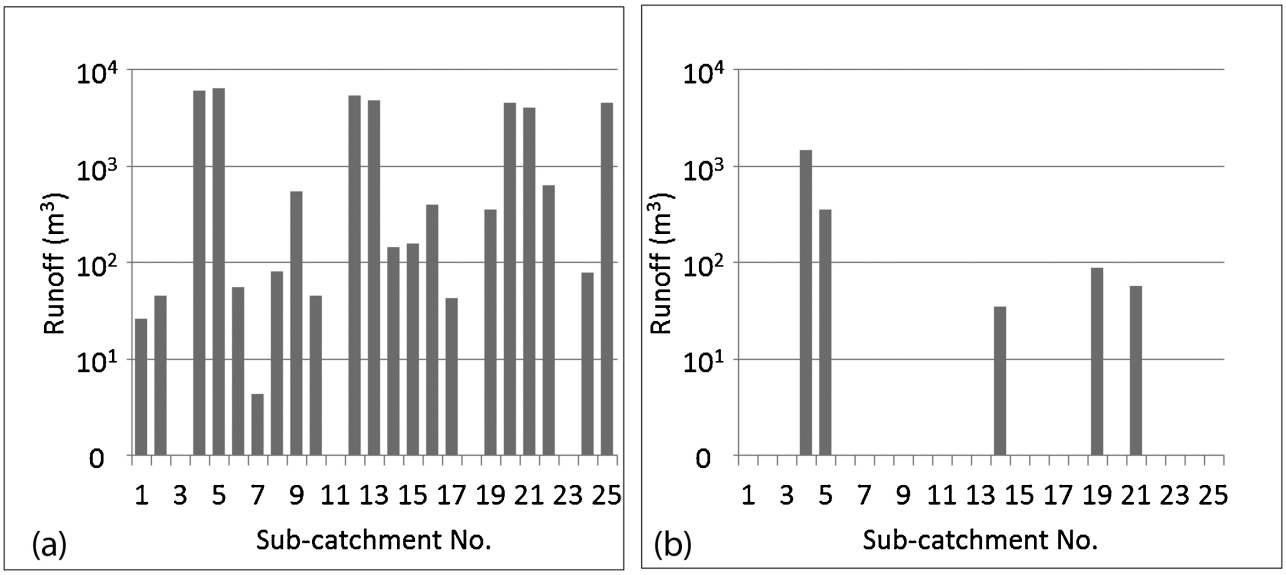

Fig. 4. Runoff (m^3) in each sub-catchment calculated using the WHCatch model for the maximum annual rainfall (a) and the threshold rainfall (b).

mum annual rainfall) will be presented to illustrate the relationship between different rains and the behaviour of RWH structures

The results of the water-harvesting model (RWH yield) for each RWH structure (storage area) for a dry, normal, and wet year are presented in Fig. 5.

The volume of water stored in the reservoir depends on the available runoff water and the water demand. When the water flows of the sub-catchments were assumed to be unrelated (Case 1), about 28 (wet year) and 8% (normal year) of the sub-catchments were able to meet the crop water requirements (Fig. 5a). Zero rain water harvested values for sub-catchments, however, indicated the inability of RWH to meet the water requirements. In these low rainfall areas, the water availability is extremely low since most of the rainwater is lost by soil surface evaporation. Therefore, the water productivity is low. These results showed the effectiveness of RWH and illustrated for the farmers how they could improve the performance of RWH by, for example, applying supplemental irrigation to compensate for the deficit in the crop water requirement. In addition, the performance of the RWH can be significantly improved, through concentrating the rainwater on part of the land. Often, one life-saving irrigation to rainfed crops at the most critical growth stage could substantially improve yield (Hachum and Mohammad, 2007). Case 2, where all sub-catchments were potentially interdependent, yielded more insight to the hydrological process in the entire catchment. Much more water will flow between sub-catchments; therefore about 44, 32, and 16% of all sub-catchments had sufficient water to meet the crop water requirements in a wet, normal, and dry year, respectively (Fig. 5b). It is observed that runoff has changed over the area according to the land use and flow direction, usually areas with a large slope tends to more runoff generation and lower infiltration rates. From case 2, it is clear that the estimated runoff volumes are high and a series of connected reservoirs may be more efficient than one large reservoir in the area. These results are in agreement with field observations (Table 1). The sub-catchments 10 and 15 for example, have poor function and maintenance values because they have received insufficient rainwater, thus leading to abandonment and dead trees. On the other hand, the trees in sub-catchments 20 and 22 (these have good scores for functioning and maintenance) are growing well. This is reflected in the results of our model presented in Fig. 5b. Zero values of rainwater harvested occurred for reasons such as insufficient storage capacity, suboptimal height of spillway, stream flow direction, siting and type of RWH adoption, and socio-economic aspects not included in this study.

From literature it can be seen that the watershed-runoff relationship in arid and semi-arid areas has long been reported and it turns out that the volume of the harvested runoff is directly proportional to the size and length of the runoff harvesting structure (Ibraimo, 2011; Li et al., 2006; Ndayakunze, 2014). Therefore, to optimize the performance of the RWH structures and to improve the yield (water availability) of the RWH system, three scenarios were applied in Case two as shown in Fig. 6

In scenario one, broken jessour (assuming values for the spillway heights of the jessr 14, 19 and 21 based on crop water requirements) were repaired. To improve the performance and safety of a RWH structure, a spillway with sufficient capacity and at the right location must be provided. Most of the RWH structures built by farmers in arid and semi-arid regions were washed away due to lack of sufficient capacity of spillways (Adham et al., 2016; Ammar et al., 2016). The WHCatch model was then applied and we analysed the performance of the 25 RWH structures. We found that all sub-catchments had sufficient water to meet the crop water requirements, showing an improvement in water availability of 56, 40 and 12% in a wet, normal, and dry year, respectively (Fig. 6b). As a second scenario we just changed the flow direction because field observations and the analysis of the water balance indicated that most of the runoff flowed in one direction (Fig. 6a). Therefore, we investigated what would happen when part of the water would flow to one sub-catchment and the remainder to another sub-catchment (Fig. 6c). Moreover, in this area the structures were built traditionally without any calculation of runoff volume and/or storage capacity. RWH structures were constructed across the flow directions, therefore there is an unequal distribution of water among these structures. The structures close to the water flow can catch more runoff by minimizing the considerable transmission losses. The WHCatch model was thus modified to have the capability to change the directions of stream flow and we analysed the performance of the 25 RWH structures. Flow directions were changed for case 2, and the water availability for the crop requirements nearly doubled for 80% of the sub-catchments in wet and normal years and in 28% of the sub-catchments in a dry year (Fig. 6d) compared to the availabilities for unchanged flow directions (Fig. 5b). In the third scenario, the scenarios one and two (change spillway heights together with changing flow directions)

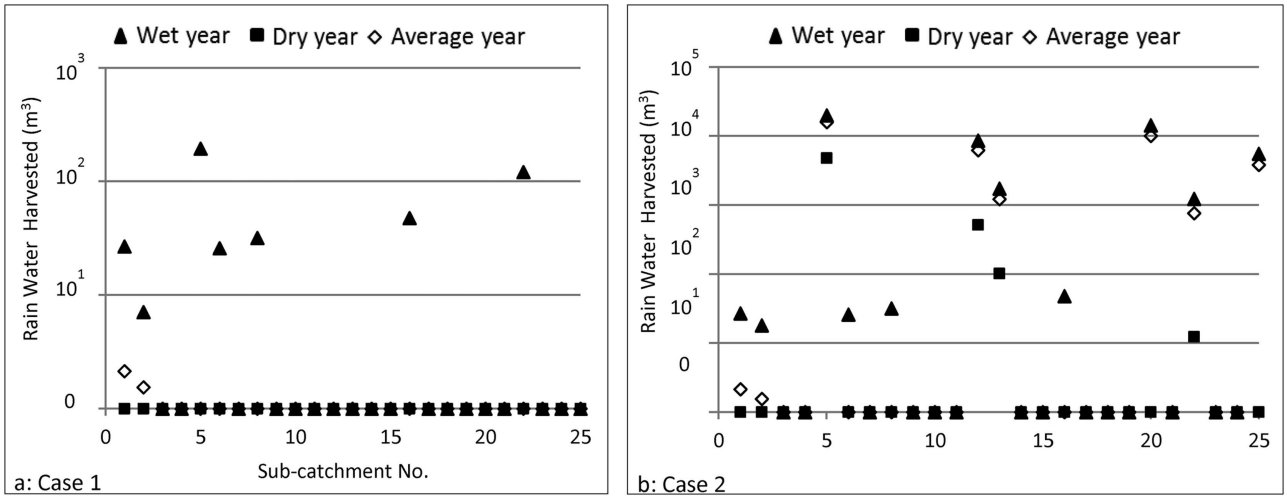

Fig. 5. Results of the WHCatch model for dry, normal, and wet years. RWH yield in each sub-catchment, (a) Case 1 (sub-catchments are independent, left) and (b) Case 2 (all sub-catchments potentially interdependent, right).

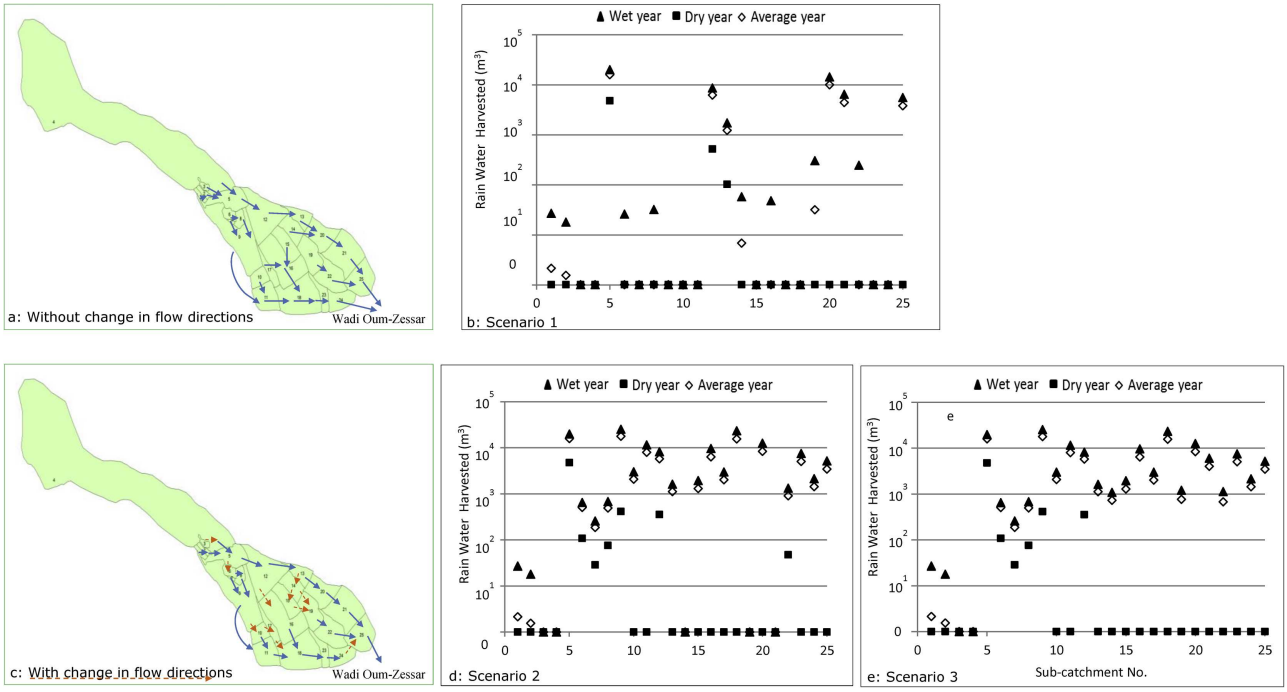

Fig. 6. The results of the optimizing model, the WHCatch model was applied for three scenarios in Case two (all sub-catchments potentially interdependent) for the dry, normal, and wet years. Sub-catchment locations with flow directions (a and c), RWH yield in each sub-catchment; (b) scenario one (changing spillway heights), (d) scenario two (changing flow directions only) and (e) scenario three combined scenarios one and two.

were combined and the performance of the 25 RWH structures was analysed (Fig. 6e). In this scenario the performance of RWH was improved increasing the efficiency of water availability for crop requirements in 92% of all sub-catchments in a wet and normal years compared to 44% for a wet year in base scenario (without changing spillway heights and flow directions). Scenario three thus had a significant impact on the performance of the RWH structures. Although the scenario's one and two improved the efficiency of the system already, the third scenario had a much higher impact and, would be an important recommendation to local farmers.

It is successfully demonstrated that changing spillway heights together with flow directions significantly enhance rainwater availability in the propose RWH solutions compared to the results of the traditional design approach. In scenario three the runoff coefficients of the connected catchments are high and the sizes of the reservoirs are adapted to the size of the contributing catchments so that water losses are minimal. In addition, rainwater harvesting systems can catch more runoff by minimizing the considerable transmission losses that take place in the outlet of the catchment (sub-catchment 25).The ability to show the frequency of runoff for each sub-catchment one of the most important options of the WHCatch model. Fig. 7 indicates which sub-catchment should have a larger storage capacity and where changing the storage capacity would have no effect.

A lot of runoff could thus be prevented by changing the storage capacity of sub-catchments 4, 14, 19, and 21 (Fig. 7a). The input data shows that this conclusion could be expected because: these structures were broken and had no storage capacity. The right side of Fig. 7b shows the times the retention areas overflowed (runoff) after changing flow direction and clearly illustrates the large impact

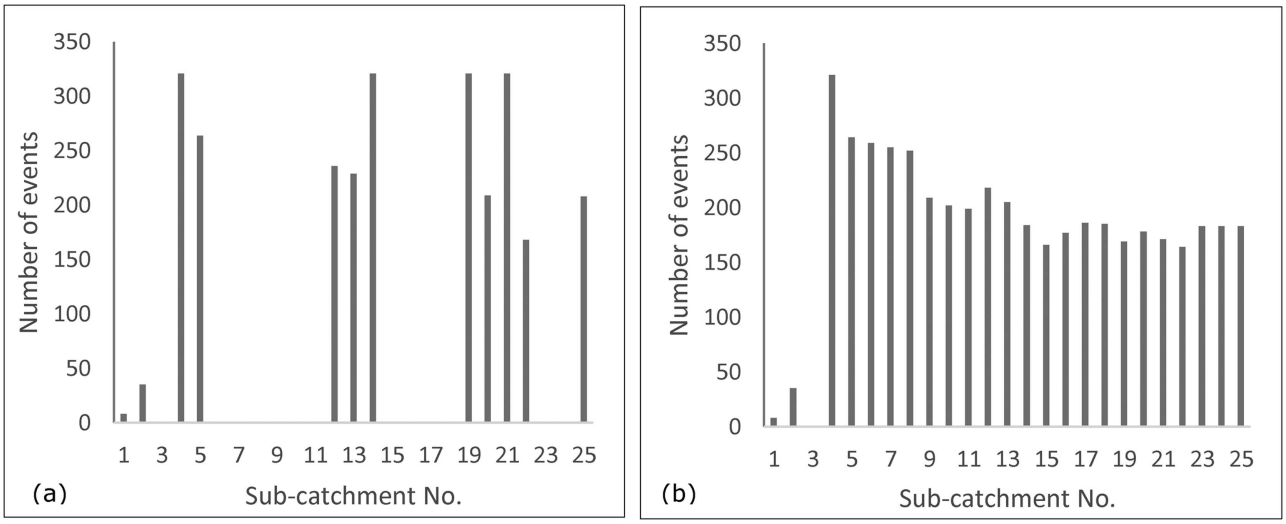

Fig. 7. Relationship between the frequency of runoff and sub-catchment number over 25 years. (a), results without changes in flow direction. (b), flow directions were changed.

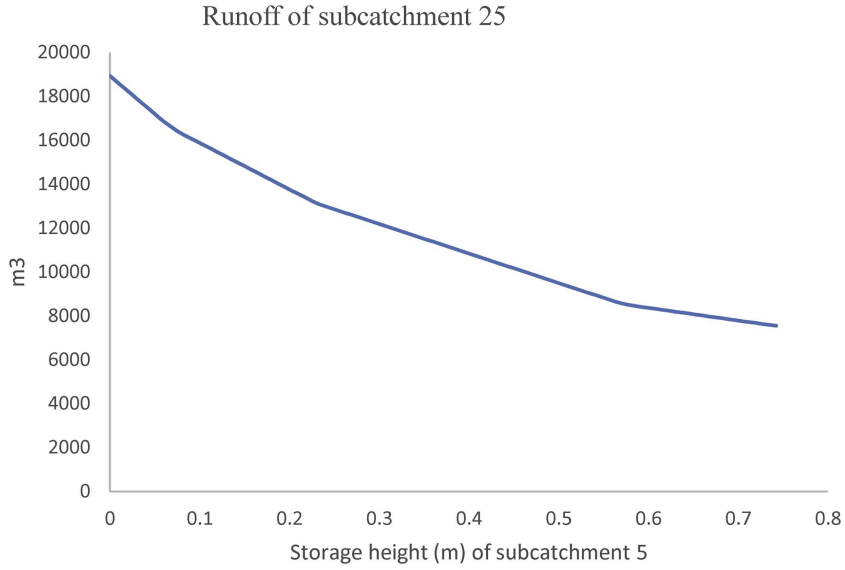

Fig. 8. An example of the impact of spillway height in a sub-catchment (5) and the runoff volume in the sub- catchments.

changing the flow direction has on the retention area. Therefore, the farmers could improve the performance of RWH structures by adapting the storage capacity and/or cultivation area to be capable of storing the amount of runoff. Then the ability of RWH to meet the water requirements will be improved. The frequency of runoffs remained unchanged only in sub-catchment 4, because this sub-catchment was considered to be a runoff area, not a storage area.

The WHCatch model can also show the influence of changing the maximum depth of water (spillway height) in a storage area on the terms of the water-balance equation for a downstream sub-catchment. An example in Fig. 8 illustrates the influence of storage height of sub-catchment 5 on the runoff from sub-catchment 25.

The slope of the line changed at a few values of storage height. The storage capacities of some downstream sub-catchments would likely be sufficiently large at these points to hold the upstream water flow. Moreover, the designer of a new RWH structure could use this model to easily estimate the storage capacity required to satisfy the crop water requirements based on the height of a spillway (Fig. 8).

The terms of the water-balance equation often need to be analysed using a GIS application such as ArcGIS, so the WHCatch model was designed to have the ability to convert the requested output data to a format readable by GIS applications. The output data can easily be imported into a GIS application and combined with a shape-file for creating maps or videos. Fig. 9, is an example of such a map, where the runoff from the catchments is shown for 1992, which is the year with maximum rainfall (117 mm).

Another interesting option of the WHCatch application is its built-in generator of precipitation events. Assuming the volumes of daily precipitation are distributed normally, the precipitation generator requires three distributions: the total yearly rainfall, the maximum rainfall in a year and the distribution of all rainfall events. Processing the rainfall data described in this paper, we obtained the following values for averages and standard deviations: 145.7 and 83.4 for the total yearly amount, 39.3 and 23.4 for the maximum value in a year and 11.4 and 13.9 for the individual events. From these distributions, values are drawn at random using the GASDEV procedure as described in (Press et al., 1987). After drawing the values from the distributions, the entire system is computed with

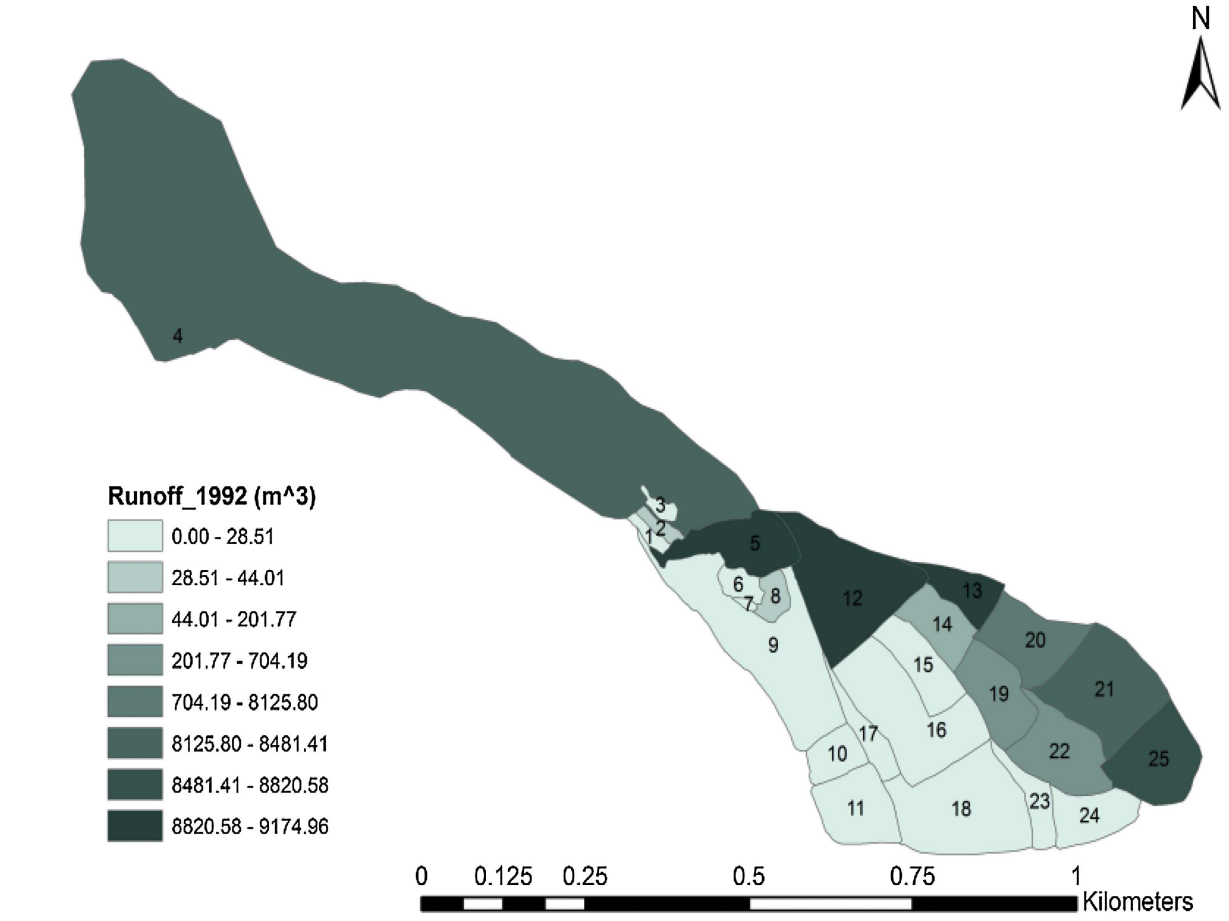

Fig. 9. An example of the runoff from the catchments for 1992.

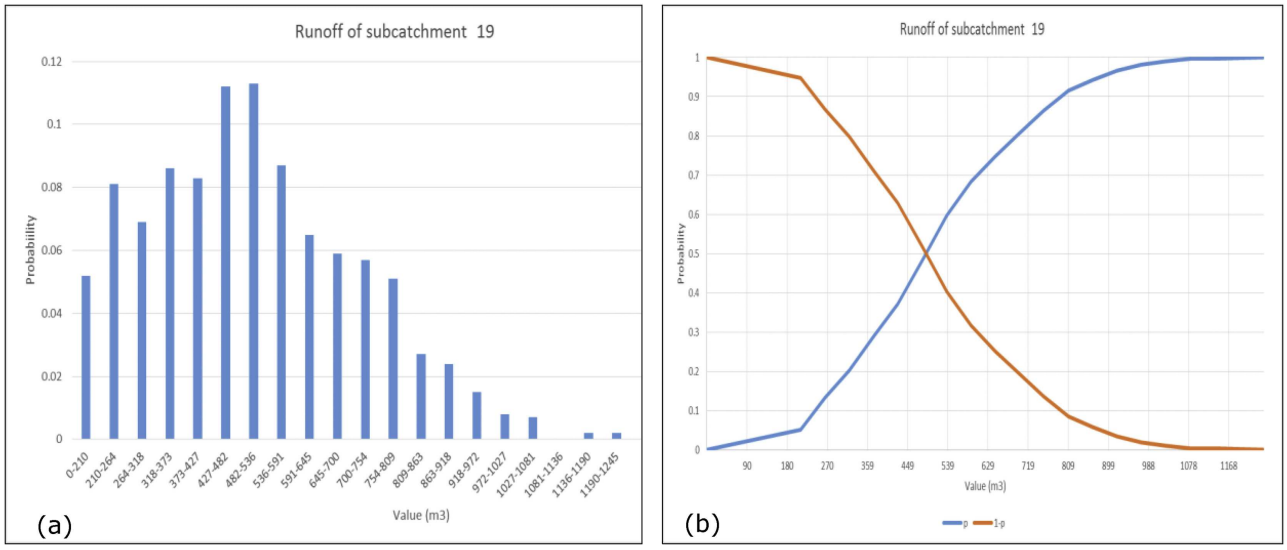

Fig. 10. The distribution of runoff obtained with 1000 years of generated precipitation events (a), and the cumulative distribution of the runoff values for sub-catchment 19, obtained from 1000 years of generated precipitation events (b). The red line indicates the probability that the runoff exceeds a certain value, the blue line is the opposite: the probability that the runoff is smaller than the corresponding value. (For interpretation of the references to color in this figure legend, the reader is referred to the web version of this article.).

these precipitation values and the water balance term of interest is read from the results and stored in memory. When all simulations a performed, a number of values are stored in memory. Defining a number of classes, the number of values in these classes can be found and the distribution of output can be drawn. As an example, we generated 1000 datasets and investigated the surface runoff volume of sub-catchment 19 (Fig. 10a).

From this figure it can be seen that most runoff values (approx. 11%) are in the classes 427–482 and 482–536 m^3. Only 5% of the values are lower than 210 m^3. From these values the program also produces a cumulative probability chart (Fig. 10b).

As an example, it can be seen from this figure that there is a 10% chance that the value of runoff will exceed 800 m^3. On the other hand, a runoff value of 1050 m^3 or higher will occur only once every 100 years. This way the simple program WHCatch can be applied for risk analysis as well.

4. Conclusions

The aim of this study was to develop a simple but generally applicable water-harvesting model and test it at sub-catchment level to evaluate and optimize the performance of RWH under different design and management scenarios. A direct approach has been chosen that can be applied with minimum data for the analysis and optimization of the performance of RWH systems. We developed a simple model, named WHCatch model, of water harvesting and applied it to characterise and quantify the terms of the water-balance equation for sub-catchments for various cases and temporal scales. The WHCatch model, a simple Excel Visual Basic for Applications macro, was developed and applied to perform all calculations and to present the results of the modelling. The WHCatch model was applied to two cases, and the main conclusions were:

- The water harvesting model results have practical importance, due to the fact that in data scarce regions lower parameterized models are advocated as they require little input data.
- Case 2 (all sub-catchments interdependent) provided an improved understanding of the hydrological processes of the entire catchment. The efficiency of RWH was nearly twice that obtained for Case 1, which assumed sub-catchment independence.
- The combination of changing the flow direction and increasing the spillway heights had a significant impact on the performance of the RWH structures. For Case 2, the water availability for the crop requirements increased in 92% of all sub-catchments compared to 44% where flow directions were not changed.
- The WHCatch model offers several options for improving the understanding of the water balance in an entire catchment, such as presenting the frequency of runoff for each sub-catchment, illustrating the influence of maximum depth of water (spillway height) in a storage area on the terms of the water-balance equation for a downstream sub-catchment, converting the requested output data to a format readable by GIS applications and generation of precipitation events to determine the runoff probability in different sub-catchments.

Overall we can conclude that this approach provides a good overview of an area and is a very useful tool to assist the planning and implementation of an RWH project, especially in arid and semi-arid regions. The scientific prediction of rains, runoff and RWH management may also be an important tool for farmers for increasing their economic returns.

However the model needs to be calibrated and tested in different regions and with various RWH techniques to validate its applicability. The socio-economic suitability/performance also need to be investigated and included in the assessment tool. These suggestions will increase the model's reliability and further generalise our methodology.

Acknowledgements

This study was conducted as part of a PhD program, with cooperation between The Higher Committee for Education Development in Iraq (HCED) and Wageningen University (The Netherlands). The field work was carried out in collaboration with the Institute des Régions Arides (*IRA*) in Tunisia. Special thanks are due to Ammar Zerrim and Messaoud Guied for their technical and field assistance. Many thanks go to Klaas Oostindie at Wageningen University and Research Center, Alterra, Soil, Water and Land Use team. This study was done under the European Union's Seventh Framework Programme (FP7/2007-2013, WAHARA project).

References

Aboukhaled, A., Arar, A., Balba, A.M., Bishay, B.G., Kadry, L.T., Rijtema, P.E., Taher, A., 1975. Research on crop water use, salt affected soils and drainage in the Arab Republic of Egypt. A review with recommendations, FAO Regional Office for the Near East, pp. 5–61.

Adham, A., Riksen, M., Ouessar, M., Ritsema, C.J., 2016. A methodology to assess and evaluate rainwater harvesting techniques in (semi-) arid regions. Water 8, 198.

Aksoy, H., Unal, N.E., Cokgor, S., Gedikli, A., Yoon, J., Koca, K., Inci, S.B., Eris, E., 2012. A rainfall simulator for laboratory-scale assessment of rainfall-runoff-sediment transport processes over a two-dimensional flume. Catena 98, 63–72, http://dx.doi.org/10.1016/j.catena.2012.06.009.

Al-Qinna, M.I., Abu-Awwad, A.M., 1998. Infiltration rate measurements in arid soils with surface crust. Irrig. Sci. 18, 83–89, http://dx.doi.org/10.1007/s002710050048.

Ammar, A., Riksen, M., Ouessar, M., Ritsema, C., 2016. Identification of suitable sites for rainwater harvesting structures in arid and semi-arid regions: a review. Int. Soil Water Conserv. Res.

Arnell, N.W., 1992. Factors controlling the effects of climate change on river flow regimes in a humid temperate environment. J. Hydrol. 132, 321–342, http://dx.doi.org/10.1016/0022-1694(92)90184-W.

Barkotulla, M.A.B., Rahman, M.S., Rahman, M.M., 2009. Characterization and frequency analysis of consecutive days maximum rainfall at Boalia, Rajshahi and Bangladesh. J. Dev. Agric. Econ. 1, 121–126.

Bhakar, S.R., Bansal, A.K., Chhajed, N., 2008. Frequency analysis of consecutive days of maximum rainfall at Udaipur. J. Inst. Eng. 89, 14–16.

Boers, T.M., Zondervan, K., Ben-Asher, J., 1986. Micro-Catchment-Water-Harvesting (MCWH) for arid zone development. Agric. Water Manage. 12, 21–39, http://dx.doi.org/10.1016/0378-3774(86)90003-X.

Bosch, van den S., Hessel, R., Ouessar, M., Zerrim, A., Ritsema, C.J., 2014. Determining the saturated vertical hydraulic conductivity of retention basins in the Oum Zessar watershed, Soutern Alterra, Wageningen/Institut des Régions Arides, Tunisia , 22, p.136.

Budyko, M.I., 1974. Climate and Life, 508 pp. Academic, San Diego Calif 72–191.

Chow, V.T., Maidment, D.R., Mays, L.W., others, 1988. Applied hydrology.

Dabral, P.P., Pal, M., Singh, R.P., 2009. Probability analysis for one day to seven consecutive days annual maximum rainfall for Doimukh (Itanagar), Arunachal Pradesh. J. Indian Water Resour. 2, 9–15.

Donohue, R.J., Roderick, M.L., McVicar, T.R., 2006. On the importance of including vegetation dynamics in Budyko's hydrological model. Hydrol. Earth Syst. Sci. Discuss. 3, 1517–1551, http://dx.doi.org/10.5194/hessd-3-1517-2006.

Durbude, D.G., Venkatesh, B., 2004. Site suitability analysis for soil and water conservation structures. J. Indian Soc. Remote Sens. 32, 399–405, http://dx.doi.org/10.1007/BF03030865.

Durbude, D.G., 2008. Estimation of probable maximum precipitation for planning of soil and water conservation structures. J. Soil Water Conserv., 7.

Gabos, A., Gasparri, L., 1983. Monthly runoff model for regional planning. Water Int. 8, 42–45.

Gebrekristos, S.T., 2015. Understanding catchment processes and hydrological modelling in the Abay/Upper Blue Nile basin. Ethiopia, http://dx.doi.org/10.1016/j.jhydrol.2013.10.006.

Gregory, J.H., Dukes, M.D., Miller, G.L., Jones, P.H., 2005. Analysis of double-ring infiltration techniques and development of a simple automatic water delivery system. Appl. Turfgrass Sci., http://dx.doi.org/10.1094/ATS-2005-0531-01-MG. Abstract.

Gupta, K.K., Deelstra, J., Sharma, K.D., 1997. Estimation of water harvesting potential for a semiarid area using GIS and remote sensing. In: Remote Sensing and Geographic Information Systems for Design and Operation of Water Resources Systems (Proceedings of the Rabat Symposium S3), IAHS Publ No. 242, pp. 53–62.

Hachum, A.Y., Mohammad, E.M., 2007. Optimal reservoir sizing for small scale water harvesting system at Al-Hader in Northern Iraq. J. Al-Rafidain Eng., 15.

Ibraimo, N.A., 2011. Rainwater Harvesting: Management Strategies in Semi-arid Areas. University of Pretoria.

Jasrotia, A.S., Majhi, A., Singh, S., 2009. Water balance approach for rainwater harvesting using remote sensing and GIS techniques, Jammu Himalaya, India. Water Resour. Manage. 23, 3035–3055, http://dx.doi.org/10.1007/s11269-009-9422-5.

Kamphorst, A., 1987. A small rainfall simulator for the determination of soil erodibility. Neth. J. Agric. Sci. 35, 407–415.

Kumar, D., Kumar, S., 1989. Rainfall distribution pattern using frequency analysis. J. Agric. Eng. 26, 33–38.

Kumar, A., Kaushal, K.K., Singh, R.D., 2007. Prediction of annual maximum daily rainfall of Almora based on probability analysis. Indian J. Soil Conserv. 35, 82–83.

Lee, C.-Y., 2005. Application of rainfall frequency analysis on studying rainfall distribution characteristics of Chia-Nan plain area in Southern Taiwan. Crop Environ. Bioinform. 2, 31–38.

Li, X.-Y., Shi, P.-J., Sun, Y.-L., Tang, J., Yang, Z.-P., 2006. Influence of various in situ rainwater harvesting methods on soil moisture and growth of Tamarix ramosissima in the semiarid loess region of China. For. Ecol. Manage. 233, 143–148.
Makungo, R., Odiyo, J.O., 2011. Determination of Steady State Infiltration Rates for Different Soil Types in Selected Areas of Thulamela Municipality, South Africa.
Ndayakunze, A., 2014. Optimising Rainfall Utilisation in Dryland Crop Production: A Case of Shallow-rooted Crops. University of Pretoria.
Ouessar, M., 2007. Hydrological Impacts of Rainwater Harvesting in Wadi Oum Zessar Watershed (Southern Tunisia). Ghent University.
Potter, N.J., Zhang, L., 2009. Interannual variability of catchment water balance in Australia. J. Hydrol. 369, 120–129, http://dx.doi.org/10.1016/j.jhydrol.2009.02.005.
Press, W.H., Flannery, B.P., Teukolsky, S.A., Vetterling, W.T., Chipperfield, J.R., 1987. Numerical recipes: the art of scientific computing: Cambridge University Press, Cambridge, 1986 (ISBN 0–521-30811-9). xx+ 818 pp. Price{\pounds} 25.00. Analytica Chimica Acta 199, 293–294.
Raes, D., Mallants, D., Song, Z., 1996. RAINBOW: a software package for analysing hydrologic data. In: Hydraulic Engineering Software VI. Computational Mechanics Publications, Southampton, Boston, pp. 525–534.
Schiettecatte, W., Ouessar, M., Gabriels, D., Tanghe, S., Heirman, S., Abdelli, F., 2005. Impact of water harvesting techniques on soil and water conservation: a case study on a micro catchment in southeastern Tunisia. J. Arid Environ. 61, 297–313, http://dx.doi.org/10.1016/j.jaridenv.2004.09.022.
Sharma, M.A., Singh, J.B., 2010. Use of probability distribution in rainfall analysis. N. Y. Sci. J. 3, 40–49.
Tadesse, N., Tadios, S., Tesfaye, M., 2010. The Water Balance of May Nugus Catchment, Tigray, Northern Ethiopia. Agricultural Engineering XII, pp. 1–29.
Tekleab, S., Uhlenbrook, S., Mohamed, Y., Savenije, H.H.G., Temesgen, M., Wenninger, J., 2011. Water balance modeling of Upper Blue Nile catchments using a top-down approach. Hydrol. Earth Syst. Sci. 15, 2179–2193, http://dx.doi.org/10.5194/hess-15-2179-2011.
Thornthwaite, C.W., 1948. An approach toward a rational classification of climate. Geogr. Rev., 55–94.
Uhlenbrook, S., Didszun, J., Wenninger, J., 2008. Source areas and mixing of runoff components at the hillslope scale—a multi-technical approach. Hydrol. Sci. J. 53, 741–753, http://dx.doi.org/10.1623/hysj.53.4.741.
Wainwright, J., 2002. The effect of temporal variations in rainfall on scale dependency in runoff coefficients. Water Resour. Res. 38, http://dx.doi.org/10.1029/2000WR000188.
Weibull, W., 1939. A statistical theory of the strength of materials (No. 151). Generalstabens litografiska anstalts förlag.
Xu, C.-Y., Vandewiele, G.L., 1992. Reliability of calibration of a conceptual water balance model: the humid case. In: The 9th International Conference on Computational Methods in Water Resources, Denver, CO, USA, 06/92, pp. 773–780.
Yang, D., Sun, F., Liu, Z., Cong, Z., Ni, G., Lei, Z., 2007. Analyzing spatial and temporal variability of annual water-energy balance in nonhumid regions of China using the Budyko hypothesis. Water Resour. Res., 43.
Yang, D., Shao, W., Yeh, P.J.-F., Yang, H., Kanae, S., Oki, T., 2009. Impact of vegetation coverage on regional water balance in the nonhumid regions of China. Water Resour. Res. 45, W00A14, http://dx.doi.org/10.1029/2008WR006948.
Zhang, Z., Chen, X., Huang, Y., Zhang, Y., 2014. Effect of catchment properties on runoff coefficient in a karst area of southwest China. Hydrol. Processes 28, 3691–3702, http://dx.doi.org/10.1002/hyp.9920.